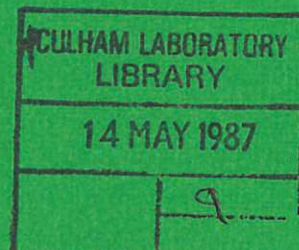




UKAEA

Preprint

CULHAM LIBRARY
REFERENCE ONLY



R

LEVEL INVERSION IN MULTIPLY CHARGED IONS AND POSSIBLE APPLICATIONS

N. J. PEACOCK

H. P. SUMMERS

CULHAM LABORATORY
Abingdon Oxfordshire

1987

This document is intended for publication in a journal or at a conference and is made available on the understanding that extracts or references will not be published prior to publication of the original, without the consent of the authors.

Enquiries about copyright and reproduction should be addressed to the Librarian, UKAEA, Culham Laboratory, Abingdon, Oxon. OX14 3DB, England.

LEVEL INVERSION IN MULTIPLY CHARGED IONS* AND POSSIBLE APPLICATIONS

N J Peacock and H P Summers⁺

Culham Laboratory, Abingdon, Oxon OX14 3DB
(Euratom/UKAEA Fusion Association)

Abstract

A survey is given of plasma conditions which are known to produce population inversion between excited states in highly ionised atoms and to lead to light amplification by stimulated XUV emission. Recent successful experiments on the use of plasma medium to generate lasing action at XUV wavelengths are reviewed and the prospects for reaching shorter wavelengths are discussed.

* Paper presented to the Conference on the Physics of Multiply Charged Ions, Groningen September 1986.

⁺ University of Strathclyde, on attachment to JET Joint Undertaking, Abingdon, Oxon. OX14 3EA. UK.

January 1987

1 INTRODUCTION

Lasers operating at X-ray wavelengths are considered to have important applications in crystallography and materials science in much the same way as synchrotron and wiggler sources are now used but with the possibility of fast time resolution arising from the transient conditions for lasing. Coherent X-ray imaging of biological (in vivo) cells makes an appealing application for lasers operating within the 'water window' ie between 23Å and 44Å, where the contrast between the absorption of the aqueous matrix and the carbon atoms of the proteins is greatest. An immediate application relates to the use of short wavelength lasers as diagnostic beam probes for interferometry, refraction and atomic species studies in laser compressed matter. A probe laser beam operating at 100Å, say, could be used up to electron densities $\sim 10^{24} \text{cm}^{-3}$, the critical density for total reflection being

$$n_{ec} \approx 10^{21} \text{cm}^{-3} / \lambda^2 (\mu\text{m})$$

This density is of the same order as has been reported for present laser compression experiments. Other applications which do not necessarily demand wavelengths as short as X-rays, include micro-manufacturing of integrated circuits and fine-scale photolithography.

After nearly two decades of research world-wide and several false starts, the search for X-ray lasers has been rewarded with several recent demonstrations of lasing action, see articles in [1] and [2] [3] [4] [5]. It is worth making clear at the outset that lasers 'operating' in the X-ray region have not yet been developed and that the recent experiments are considerably more modest in their claims, namely a demonstration of the amplification of extreme ultra-violet (XUV) light by stimulated emission. The present short review draws attention to the factors which have provoked the success of the recent experiments and speculates on possibilities for reaching higher photon energies.

In principle, lasing at X-ray wavelengths involves either valency electron transitions in highly ionised atoms or inner-shell, eg, K- or L- shell excitation of weakly ionised atoms. In practice it is difficult, perhaps impossible, to achieve the density of ions or atoms with inner-shell vacancies required for lasing without at the same time generating a plasma. More typically, the large energy input required to distort the level population from their 'thermal' or equilibrium values ensures that the plasma environment is highly ionised.

Normally, level populations are heavily weighted in favour of the ground state, the occupancy of the upper levels scaling approximately as $\frac{1}{n^3}$ where n is the principle quantum number. Absorption and spontaneous emission are the only photon transfer process to worry about.

In the event that the levels are inverted, then stimulated emission plays a role as can be seen from the equation governing radiation transfer from a plasma (with vector normal \tilde{n}).

$$\tilde{n} \cdot \text{Grad } I_\nu(r, \theta) = J_\nu(r) - k_\nu(r) I_\nu(r, \theta) \quad (1)$$

and where the emission coefficient $J_\nu(r)$ is

$$J_\nu(r) = \frac{h\nu_0}{4\pi} A_{u\ell} N_u(r) \phi_{u\ell}(\nu, r) \quad (2)$$

and the absorption coefficient

$$k_\nu(r) = \frac{h\nu_0}{4\pi} B_{\ell u} g_\ell \left[\frac{N_\ell(r)}{g_\ell} - \frac{N_u(r)}{g_u} \right] \phi_{\ell u}(\nu, r), \quad (3)$$

where the absorption and emission profiles $\phi(\nu, r)$ when intergrated over frequency have the value of unity.

The output intensity depends on the level populations N_u, N_ℓ and in order to gain amplification by negative absorption (ie stimulated emission), then $\frac{N_u}{g_u} > \frac{N_\ell}{g_\ell}$. Thus the inversion factor

$$F = \left[1 - \frac{N_\ell}{N_u} \frac{g_u}{g_\ell} \right] \text{ must be positive.} \quad (4)$$

Since $h\nu \frac{B_{\ell u}}{4\pi} = \pi r_0 c f_{\ell u}$, then the linear gain coefficient

$$-k \text{ (cm}^{-1}\text{)} = \pi r_0 \frac{c f_{\ell u}}{\Delta\nu_{u\ell}} \frac{g_\ell}{g_u} N_u F = \sigma_{\text{st.em.}} N_u F. \quad (5)$$

Expressing the light gain by stimulated emission as $e^{\alpha L}$, where α is now a positive quantity associated with a positive F , and L is the optical path length, then for an amplification factor $\frac{e^{\alpha L}-1}{\alpha L} \sim 10^3$,

$$\alpha L = 9 = \sigma_{\text{st.em.}} N_u F L \quad (6)$$

Assuming $\frac{\Delta \nu}{\nu_0} = 10^{-4} \rightarrow 10^{-3}$ and the absorption oscillator strength, $f_{lu} \sim 0.1$; then $\sigma_{\text{st.em.}} = 10^{-16} \rightarrow 10^{-15} \text{ cm}^2$ and if $F \approx 1$ and $L = 1$ then, $N_u \approx 10^{16} \rightarrow 10^{17} \text{ cm}^{-3}$ and this is the order of the inverted population density needed for substantial single pass gain through a plasma with a dimension $\sim 1 \text{ cm}$. At first sight the attainment of these order of magnitude figures does not look a formidable task. A major consideration however is the power required to maintain the inversion even for a transient period. The minimum pump power requirement per unit gain, can be expressed in terms of $\frac{P_{\text{(pump)}}}{\text{Area}} = N_u L h \nu (\Gamma + A_{ul})$, where $(\Gamma + A_{ul})$ represents the total spontaneous decay due to radiation (A) and radiationless processes (Γ), and hence

$$\left[\frac{P_{\text{pump}}}{\text{Area}} \cdot \frac{1}{\alpha L} \right] \propto \nu^4 \approx Z^8. \quad (7)$$

Thus a laser operating at 10Å requires a factor of 10^{12} increase in pump power over that needed to generate lasing at $1\mu\text{m}$.

A highly ionised plasma which is both produced and pumped by the most intense source available, namely a high powered (Nd) glass laser, is a suitable starting point for X-ray laser research, [6] [7] [8].

The next problem relates to the plasma conditions which are necessary to distort the level populations from their equilibrium values. The steady-state populations in hydrogenic ions [9], [10] under different conditions of ionisation and recombination provides an answer. In

strongly recombining plasmas, population inversion can occur between the lowest excited levels which are emptied by rapid radiative decay to ground and the upper neighbouring levels which are filled through recombination from the continuum states.

This situation is illustrated in Fig 1 where one would expect to find overpopulation of the $n = 3$ levels relative to $n = 2$ and hence the potential for lasing on the $H\alpha$ transitions. Inversion is a natural consequence in any strongly recombining plasma whether the recombination process is dielectronic, collisional-radiative or charge transfer recombination. The latter process, being state selective, is attractive since the upper levels can be populated directly. A sample calculation of the level populations in an Fe^{+14} ion produced by dielectronic recombination [11] is shown in Fig 2. The populations b_n are expressed as a fraction of their Saha Boltzmann equilibrium populations for a number of electron densities at a temperature of 10^6 K. Where the curves have a positive slope, level inversion occurs. At the highest densities, the recombination coefficient is decreased and collisional coupling between the levels ensure a destruction of the inversion. Of course, in laser-produced plasmas, the density is much higher but the principle remains the same, namely that in a strongly recombining plasma where collisional excitation and optical pumping (eg due to opacity) are negligible, then overpopulation occurs.

Other plasma conditions have been proposed for inversion, for example photon pumping schemes, such as resonance photon absorption or inner-shell photoionisation. Strong electronic excitation arising from a rapid increase in the plasma temperature is another possibility. It is the authors' opinion however that the recombination schemes, so far, are the most convincing and best documented scenarios for inversion in a highly ionised plasma medium.

A sample of the collision processes which can create or destroy inversion is shown in Fig 3. Clearly, a realistic calculation of the inversion requires many levels to be taken into account simultaneously. Metastable levels often play a particularly important role in the excited level populations of non-hydrogenic species. The atomic physics problem is formidable enough with often inadequately known rate processes being included in the manifold of time dependent equations describing the level populations. The complexity introduced by the plasma dynamics and radiation transfer makes a faithful (numerical) model of the inversion very difficult to construct.

The few numerical calculations which have been developed are extremely useful for predicting the general features of gain conditions, though they are usually less successful in accounting for the detailed time histories of the line intensities.

The remainder of the paper focuses on the recent plasma experiments where inversion has been shown unambiguously. We omit therefore many optical pumping and other state-selective experiments which may yet prove rewarding. For a wider discussion of the problem the reader is referred to review articles eg., by Hagelstein [12] and Key [13].

2 EXPERIMENTS ON INVERSION

Gain due to stimulated emission yields an increased brightness which in principle can be demonstrated by non-linear amplification of the light intensity with the length of the lasing medium, spectral line narrowing or reduced divergence. Non-linear amplification is the most practical of these components of the brightness since in the XUV region with diffraction grating spectrometers, the spectral line width is usually dominated by the instrument resolution and in high density plasmas the divergence is often affected by refraction due to the plasma density gradients. For this reason some care is taken to generate cylindrical plasmas with a large aspect ratio (λ/r), and with very uniform plasma conditions per unit length along the cylindrical axis.

The irradiance of the light ($\text{photons cm}^{-2}\text{s}^{-1}$) when viewed along the length of the cylinder is greater than the transverse irradiance by the ratio

$$\frac{I(\lambda)}{I(r)} = \frac{1}{\alpha L} (e^{\alpha L} - 1), \quad (8)$$

both quantities $I(\lambda)$, $I(r)$ having been 'normalised' by dividing by the longitudinal and transverse viewed plasma volumes. For small gain coefficients in the range $1 \leq \alpha L \leq 3$, the intensity ratio is difficult to interpret unambiguously in terms of stimulated emission. In the region $3 \leq \alpha L < 10$, there is a clear exponential increase in the amplified light with plasma length. For high gain coefficients, $\alpha L > 15$, typically, saturation of the stimulated emission occurs during a single pass. Clearly a demonstration of the lasing action requires $\alpha L > 3$.

There are three main reasons for the recent observations of XUV light gain, [1] [2] [3] [4] [5]. These are improved techniques for producing long (≥ 1 cm) uniform, high temperature plasmas. Secondly, developments in time-resolved diagnostic instrumentation, and lastly the development of numerical models in which the atomic physics is coupled to the plasma dynamics.

2.1 Recombination into Hydrogenic Ions

The freely expanding plasma plume formed by irradiation of solid surfaces with a powerful visible laser has been used for over a decade to study inversion in strongly recombining conditions. Sufficiently far from the target surface, typically 1 mm or more, adiabatic cooling due to the rapid expansion causes the levels to be populated purely by a recombination cascade from the continuum. Experiments have mostly involved the populations of Rydberg levels in H-like ions since naked ion plasmas (eg. C^{6+}) are readily produced at solid surfaces with moderate irradiation intensities. Line focus irradiation of thin (micron thick) foils and of fibres have been modelled extensively [14] in order to optimise the gain, usually on the $H\alpha$ transition. These calculations have been backed up by carbon fibre irradiation experiments [4] shown schematically in Fig 4.

Gain coefficients $\sim 2-4\text{cm}^{-1}$ and $\alpha L = 4$ have been measured [4] [13] for the $H\alpha$ line of CVI at 182.2\AA , when the electron density has transiently fallen to $n_e \sim 2 \times 10^{19}\text{cm}^{-3}$ and the electron temperature to $T_e \sim 30\text{ eV}$. Evidence for gain is derived from the the longitudinally and transversely viewed intensities of the CVI Balmer series [4]. The 182.2\AA $H\alpha$ line intensity increases exponentially with plasma length while the H line at 120.5\AA remains only linearly dependent. This approach to γ -lasing in the XUV has been extended to higher Z elements eg fluorine where gain on $H\alpha$ F IX has been detected [15] at 81\AA . This is the shortest wavelength at which gain has been reported so far. Scaling to even shorter wavelengths using adiabatic expansion has been considered [13]. Unfortunately, the ideal plasma parameters [9] [10] required to keep the gain constant with increasing Z, correspond inexactly with the plasma parameters resulting from irradiation of higher Z targets. In order to create supercooled naked ion plasmas at higher Z, higher laser pump intensities are required with more rapid, possibly enhanced cooling, resulting in a shorter gain duration $\sim 20 \rightarrow 30\text{ ps}$. Higher initial densities can in principle be created with a shorter wavelength for the pump laser while cooling may be enhanced with radiating dopants. It is thought possible using this route to reach H_{α} of Al XIII at 39\AA ie., within the 'water window'.

An interesting variant of the free expansion recombination scheme, namely a stagnated expansion, using magnetic fields, has been studied by Suckewer et al. [5]. The concept here is to use magnetic fields ~ 9

Tesla to suppress the radial expansion of a cylindrical (carbon) plasma to prolong the inversion period. Cooling especially of the outer region of the plasma is ensured by radiation loss. Anomalous transport of the C^{6+} ions from the core to the outer cooled region results in recombination and inversion. Gain coefficients $\alpha L \sim 6.5$ with $\alpha \sim 6 \text{ cm}^{-1}$ have been reported for $H\alpha$ CVI at 182\AA . Gain sets in at lower density $\leq 6 \times 10^{18} \text{ cm}^{-3}$ and lasts longer, $\tau_g \sim 100 \text{ ns}$, than is the case for free plasma expansion. Evidence for gain comes from the exponential dependence of the intensity of $H\alpha$ CVI. Use of a 12% reflector at 182\AA allowed a double pass amplification of 120% of single pass signal, confirming the gain coefficient.

2.2 Li-like Ions

Free expansion cooled, laser-produced plasma have also been studied by Jaeglé and colleagues [1] [3]. In these experiments however, recombination of He-like ions eg Al XII are calculated to form excited states of Al XI with inversion between the lower 3d and the upper 4f and 5f levels. The recombination mechanism is dielectronic.

The line intensity emitted from plasma columns of differing lengths but with identical plasma parameters is used to diagnose the gain

$$\frac{I_L}{I_\ell} = \frac{1 - e^{-kL}}{1 - e^{-k\ell}} \quad (9)$$

where the linear gain coefficient $\alpha = -k (\text{cm}^{-1})$.

The Al XI, 3d - 4f line at 105.7\AA shows transiently an anomalous behaviour relative to neighbouring lines in the respect that the absorption is negative with $\alpha \approx 2 \text{ cm}^{-1}$. Opacity between the ground states and the 3d levels may prove to be an ultimate problem with this scheme.

2.3 Neon-like Ions

The most convincing XUV gain experiments have been reported for Neon-like ion species for example, Se XXV, [1] [2]. Lasing takes place between the metastable $2s^2 2p^5 3p$ levels and the lower $2s^2 2p^5 3s$ levels, the latter having strongly allowed decay rates to ground, Fig 5. The $J = 0$, $2p^5 3p$ levels can be populated by non-dipole electron excitation directly for the $2p^6 1S_0$ ground state, whereas the $J = 2$, $2p^5 3p$ levels are most likely to be populated by cascades from higher levels. Dielectronic recombination would favour the $J = 2$ states.

Numerical models [2] based on purely collisional excitation and radiative depopulation predict the $J = 1$, $2p^5 3s \leftarrow J = 0$, $2p^5 3p$ transitions, which have the highest A_{ul} values within the multiplet, to show the most gain following inversion. In fact, the $j = 2$, $2p^5 3p$ transitions are observed, Fig 5, to have the higher (x5) gain over the other transitions though there is also a measurable gain on all the other decays between $3p$ and $3s$. The inversion mechanism may not be collisional excitation as first thought [2] but could indeed be a recombination laser in common with the other demonstrations of XUV gain described earlier in this paper.

Dielectronic recombination happens to be the most important recombination process in the formation of the highly ionised neon-shell ions. The population rate of the $2p^5 3p$ levels via the doubly-excited states formed by dielectronic recombination of fluorine-like Se has been included recently in the gain calculations of Hagelstein et al. [16] and of Jacquemot et al. [17]. The dielectronic rates for Se XXV have also been calculated by Summers et al. [18] and we note, see Fig 6, that recombination directly into the $2p^5 3p$ configuration greatly favours the multiplets with the higher statistical weights. The results of including recombination [16] is to equalise the $J = 2$ and $J = 0$ gains while in [17] the $J = 2$, $2p^5 3p$ levels are predicted to have the higher gains.

Starting from the viewpoint that the neon-shell lasing is purely a recombination process we indicate, table 1, the population rates into the $2p^5 3p$ levels, which may be derived from Fig 6 by assuming a statistical population among J states, and, multiplying these rates by the A_{ul} values gives a crude ordering of the gain coefficients for each transition. Table 1 indicates also that there is a great deal of level 'impurity' and that spectroscopic assignments are something of a problem.

The purely recombining scheme, table 1, indicates that the $2p^5 3p \ ^3D_3$ and $\ ^3D_1$ levels should have a strong or appreciable decay to $2p^5 \ 3s$. These lines might at first sight not be expected to lase since their lower levels $2p^5 3s \ ^3P_2$ and $\ ^3P_0$ respectively appear metastable. However quadrupole collisional mixing of the $3s$ levels at the high plasma ion density probably quenches the metastability.

The $2p^5 3p \ ^3D_2$ (30% $\ ^1D_2$) and $\ ^1S_0$ (20% $\ ^3P_0$) are the next most important lines of which only the former is observed to lase strongly. The strongest observed lasing line from the $2p^5 3p \ ^3P_2$ (32% $\ ^1D_2$) level comes next in order in the table.

TABLE 1

Se XXV, 3s-3p DIELECTRONIC LINE 'EMISSION RATES'

$\lambda(\text{\AA})$		$\langle \sigma v \rangle_d \cdot A(s^{-1})$	$2J+1$
211	$2p^5 3s \ 3p^2$ - $2p^5 3p \ 3D_3$	$1.77 \times 10^{-12} \times 1.45 \times 10^{10}$	2.57×10^{-2} 7
*209.6	$2p^5 3s \ 3p^1$ (39% $1P_1$) - $2p^5 3p \ 3D_2$ (36% $1D_2$)	$1.1 \times 10^{-12} \times 1.5 \times 10^{10}$	1.65×10^{-2} 5
182.4	$2p^5 3s \ 3p^1$ (39% $1P_1$) - $2p^5 3p \ 1S_0$ (20% $3P_0$)	$4 \times 10^{-13} \times 2.5 \times 10^{10}$	1.0×10^{-2} 1
113.3	$2p^5 3s \ 1P_1$ (39% $3P_1$) - $2p^5 3p \ 1S_0$ (20% $3P_0$)	$4 \times 10^{-13} \times 2.3 \times 10^{10}$	9.2×10^{-3} 1
*206.3	$2p^5 3s \ 1P_1$ (39% $3P_1$) - $2p^5 3p \ 3P_2$ (32% $1D_2$)	$6.61 \times 10^{-13} \times 7.6 \times 10^9$	5.0×10^{-3} 3
263	$2p^5 3s \ 1P_1$ (39% $3P_1$) - $2p^5 3p \ 1D_2$ (54% $3D_2$)	$1.07 \times 10^{-12} \times 4 \times 10^9$	4.3×10^{-3} 5
169	$2p^5 3s \ 1P_1$ (39% $3P_1$) - $2p^5 3p \ 3P_0$ (20% $1S_0$)	$1.58 \times 10^{-13} \times 2.6 \times 10^{10}$	4.1×10^{-3} 1
207.5	$2p^5 3s \ 3P_0$ - $2p^5 3p \ 3D_1$ (57% $3P_1$)	$3.5 \times 10^{-13} \times 9.8 \times 10^9$	3.4×10^{-3} 3

* Lasing transitions [2]. Identifications corroborated by Cogordan and Lunell. Physica Scripta 33, 406-411 (1986).

Clearly the ordering of the 'emission rates' (in table 1) is not in accord with the experimental results, Fig 7. The problem with the pure recombination model is not so much the presence of the observed lasing lines but absences including $3s\ 1P_1 - 3p\ 1S_0$ and $3s\ 3P_2 - 3p\ 3D_3$. This latter line especially presents a difficulty. However two points must be noted. Firstly, the identification of all line components is not yet confident. Overlap and misinterpretation are still possible. Secondly, rough estimates of positive ion collisionally induced quadrupole mixing rate of the $3D$ levels indicate that they are comparable with $3s-3p$ A values. This opens the possibilities of funnelling of the emission through a restricted number of lasing lines. An additional factor for $J=2$ (and $J=3$) levels is the population rate via recombination from $2p^5 3d$, Fig 5. The dielectronic rates into the $2p^5 3d$ levels are higher even than into the $3p^5 3p$ term and favour the $3F$, $3D$ multiplets which decay directly into the upper levels of the lasing transitions, table 1. The $2p^5 3p\ 1S_0$ level lacks this populating mechanism since the $2p^5 3d$ levels feeding $2p^5 3p\ 1S_0$ have branching decays to ground. A detailed study of this recombination model remains to be done.

In the Lawrence Livermore Laboratory (LLL) experiments a uniform $1 \rightarrow 2\text{ cm} \times 200\ \mu\text{m}$ plasma is initially produced by a 450 ps duration irradiation pulse on foil targets, one such foil, for example, being $0.15\ \mu\text{m}$ formvar coated with 750\AA of Se. Using green light with a pump intensity $\sim 5 \times 10^{13}\text{ W cm}^{-2}$, neon-like ions from elements in the range $Z \approx 30 \rightarrow 40$ are readily produced. The results of using different plasma gain lengths to study emission from Se XXV and neighbouring ion species, are illustrated in Fig 7. The linear gain coefficient on the $J=1, 2p^5\ 3s \leftarrow J=2, 2p^5\ 3p$ line is $\sim 5 \rightarrow 6\text{ cm}^{-1}$, with a considerably smaller gain on the $J=1 \leftarrow J=0$ transition. Lasing on a single pass is unambiguously demonstrated.

The period of lasing emission appears to follow close in time to the switch-on of the laser pump when the electron temperature is high, $T_e \sim 800\text{ eV}$. This coincidence would not discount dielectronic recombination, in contrast to other recombination processes, as a mechanism for creating the inversion.

Experiments at LLL with longer plasma gain lengths have led to sufficiently high gain coefficients, $\alpha L \geq 15$, to induce saturation during a single pass. Isoelectronic extrapolation of the inversion scheme has also been demonstrated [1] by lasing in Y XXX at 155\AA and 157\AA and in Mo XXXIII at 131\AA and 133\AA , the shortest lasing line observed being at 106\AA .

At the upper limit of the plasma lengths (~ 4.5 cm) studied in these experiments, Mathews et al. [1], refraction of the amplified light out of the plasma volume proves to be the limiting factor in the gain length and in the angular divergence (~ 10 mrad) of the lasing light.

Scaling the 3p to 3s inversion in neon-like ions to still higher Z appears to present no unsurmountable difficulties up to $Z = 47$ ie Ag XXXVIII, lasing at 99Å. The enormous pump power required for still higher Z and shorter wavelengths becomes a problem however and the inversion analogue with the 4d and 4p levels of Ni-like ions may be more promising. Other analogue ion species, for example, BeI-, BI- and CI - like ions where inversion might also be expected between the excited 3s and 3p levels have been modelled by Feldman and co-workers, [19] [20].

3. DISCUSSION AND SUMMARY

A measure of the relative quantum efficiency of different lasing schemes is the lasing energy relative to the excitation energy of the upper levels [13]. This is illustrated in Fig 8. On this basis, the Li-like ion and the H-like ion recombination schemes have a higher quantum efficiency than the Neon-like ions and so are more suited for scaling to higher lasing photon energies. The present state of the experiments on each of these ion species is summarised in the caption to Fig 8.

There are strong indications that the inversion successfully achieved with all of these ion species is basically due to a recombination process.

These break-through experiments are very recent and many corroborative experiments and improvements remain to be carried out. The maximum lasing power achieved is ~ 1 MW with a very low over-all efficiency $\sim 10^{-7}$. Rapid progress can be anticipated using oscillator-amplifier and confocal mirror configurations. Plasma profiling may also play an important role.

ACKNOWLEDGEMENTS

In this short review the authors have omitted many of the early seminal contributions. It is a pleasure to acknowledge the many helpful discussions with the enthusiasts in this research area. These have included M H Key and O Willi of Rutherford Appleton Laboratory; G J Pert from Hull University, P Jaeglé and his associates at Orsay and Palaiseau, D L Mathews and P Hagelstein from the Lawrence Livermore Laboratory, R C Elton from the Naval Research Laboratory and S Suckewer from the Princeton Plasma Physics Laboratory.

REFERENCES

- [1] Proceedings of International Colloquium on X-ray Lasers, Aussois (France) April 14-17, 1986. Publ. Jnl de Physique. Colloque C6, Supplement to No 10, Vol 47. (1986).
- [2] Mathews D L, Hagelstein P L. et al., Phys. Rev. Lett., 54, 289, (1985).
- [3] Jaeglé P, Carillon A et al. Europhys. Lett., 1, 555, (1986).
- [4] Key M H et al. see [1], C6-71.
- [5] Suckewer S, Skinner C H et al. Phys. Rev Lett., 55, 1753, (1985).
- [6] Irons F E and Peacock N J. J Phys B Atom Molec. Phys. 7, No 9 1109 (1974).
- [7] Elton R C Applied Optics 14, No 1, 97, (1975).
- [8] Ilyukhin A A, Perehudov G V, Ragozin E N, Sobelman I I and Chirkov V A. JETP Letters, 25, 535 (1977)
- [9] McWhirter R W P and Hearn A G. Proc. Phys. Soc. 82, 641, (1963).
- [10] Johnson W C and Hinnov E. Jnl Quant Spect. and Rad. Transfer. 13, 333 (1973).
- [11] Burgess A and Summers H P. Astrophys. Jnl. 157, 1007, (1969).
- [12] Hagelstein P L. 'Review of Short Wavelength Lasers'. proc. 9th Int. Conf. on Atomic Physics, Seattle. Wash. USA (1984), pp 382 (editors R S Van Dyk and E N Fortson) Publ. by World Scientific Publ. Singapore (1984). Also Livermore Laboratory Report UCRL-92336 (1985).
- [13] Key M H. 'X-ray lasers - A survey of Progress World Wide.' Paper presented to CLEO meeting USA (1986).
- [14] Pert G J. see [1], C6-177.
- [15] Willi O et al. Proc 30th Annual Technical Symposium on optics and optical electronics in Applied Science and Engineering. San Diego, Aug 1986.
- [16] Hagelstein P L, Rosen M D and Jacobs V L. Livermore Laboratory Report. UCRL-94378 (1986). Submitted Phys. Rev. A (1986).
- [17] Jacquemot S, Berthier E, Vuillemin M and Cornille M. see [1] C6-339.
- [18] Summers H P, Behringer K H and Wood L to be published, Physica Scripta (1986). Also JET reprint JET - P(86) 36. (1986).
- [19] Feldman U, Seely J F and Bhatia A K., Jnl. Appl. Phys. 56, 2475. (1984).
- [20] Feldman U, Seely J F and Doschek G A, see [1] C6-187. (1986).

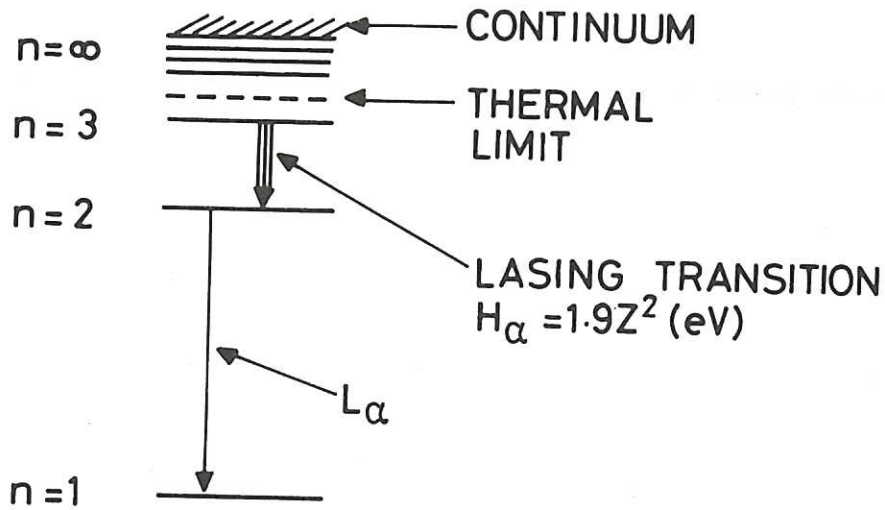
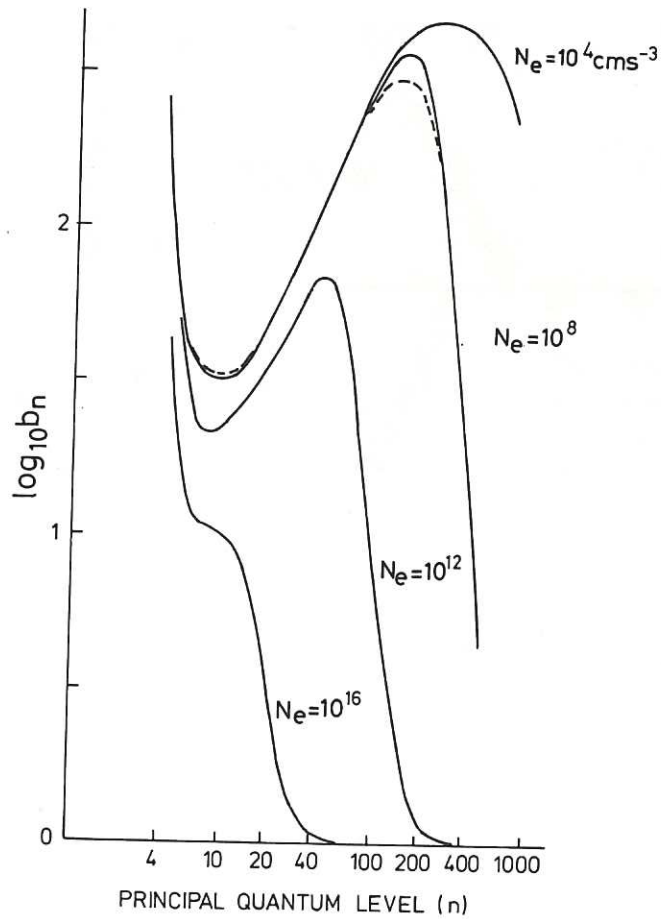


Fig.1 Basic energy level scheme of recombining H-like ion indicating lasing transitions below the thermal limit.



Fe^{+14} LEVEL POPULATIONS FOR $T_e = 2 \times 10^6 \text{ K}$

Fig.2 Steady state population of principal quantum levels for Fe^{+14} ions in recombining plasmas with electron densities n_e varying from 10^4 cm^{-3} to 10^{16} cm^{-3} and with $T_e 2 \times 10^6 \text{ K}$. The level populations b_n are expressed as a fraction of their Saha-Boltzmann equilibrium values^[11].

Populating and de-populating processes in XUV lasing ion.

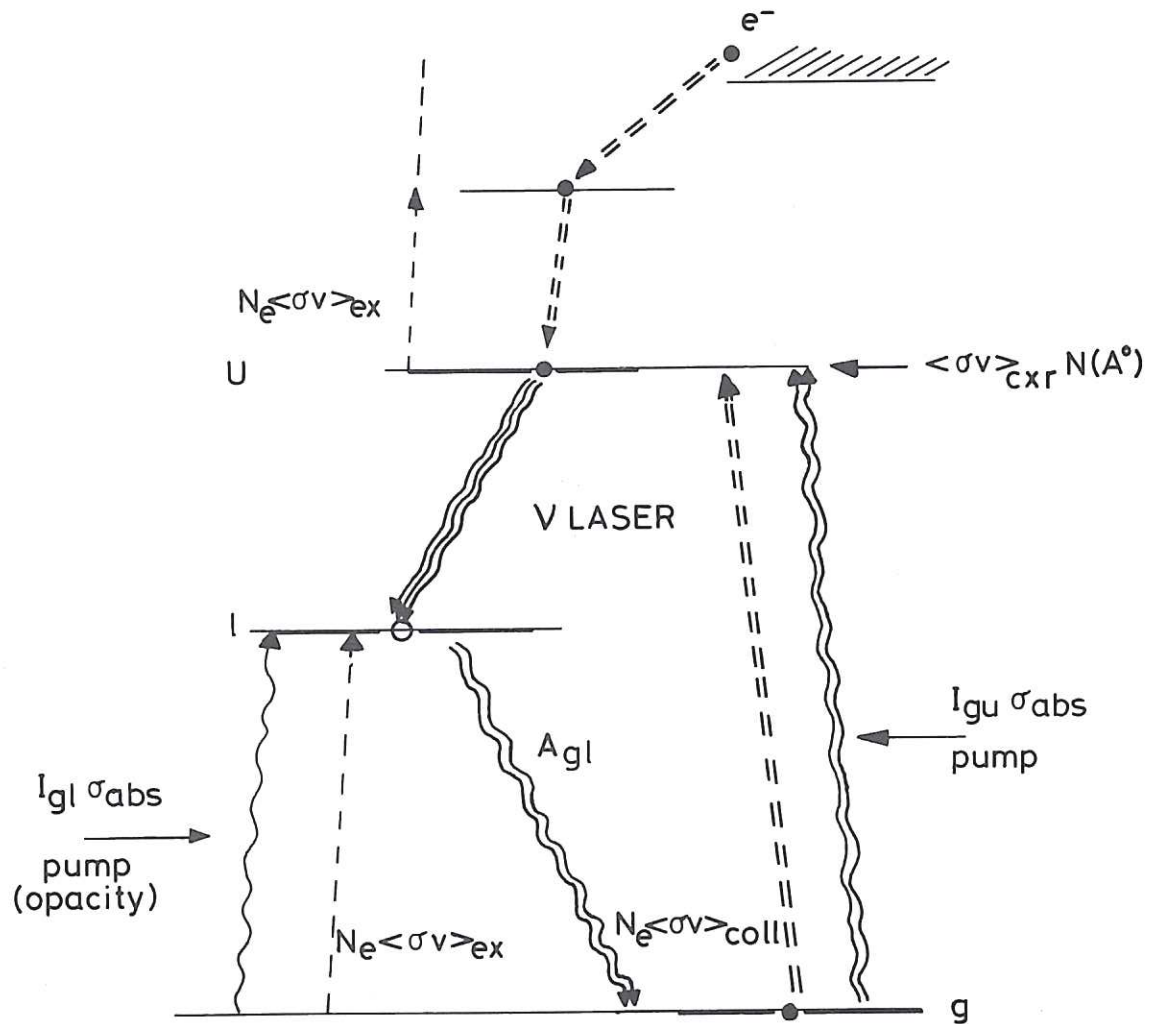


Fig.3 Schematic representation of populating and de-populating processes in an XUV lasing ion. $n_e \langle \sigma v \rangle_{ex}$, $n_e \langle \sigma v \rangle_{coll}$ represent the electronic excitation and de-excitation rates respectively with n_e the electronic density. $\langle \sigma v \rangle_{CXR} N(A^0)$ is the product of the atomic density $N(A^0)$ of atoms A^0 and the charge exchange recombination rate $\langle \sigma v \rangle_{CXR}$ into the upper level of the lasing transition. The thin (single) lines denote the processes destroying inversion; the thicker (double) lines represent inversion creative processes and the thickest (triple) lines represent the lasing transition.

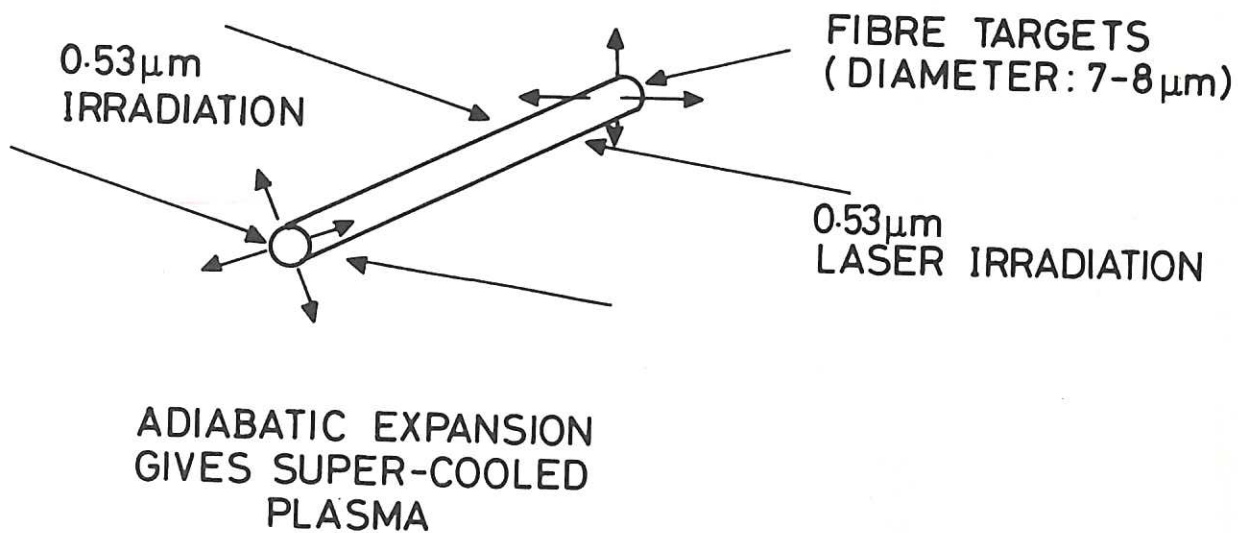


Fig.4 Schematic of free-expansion laser.

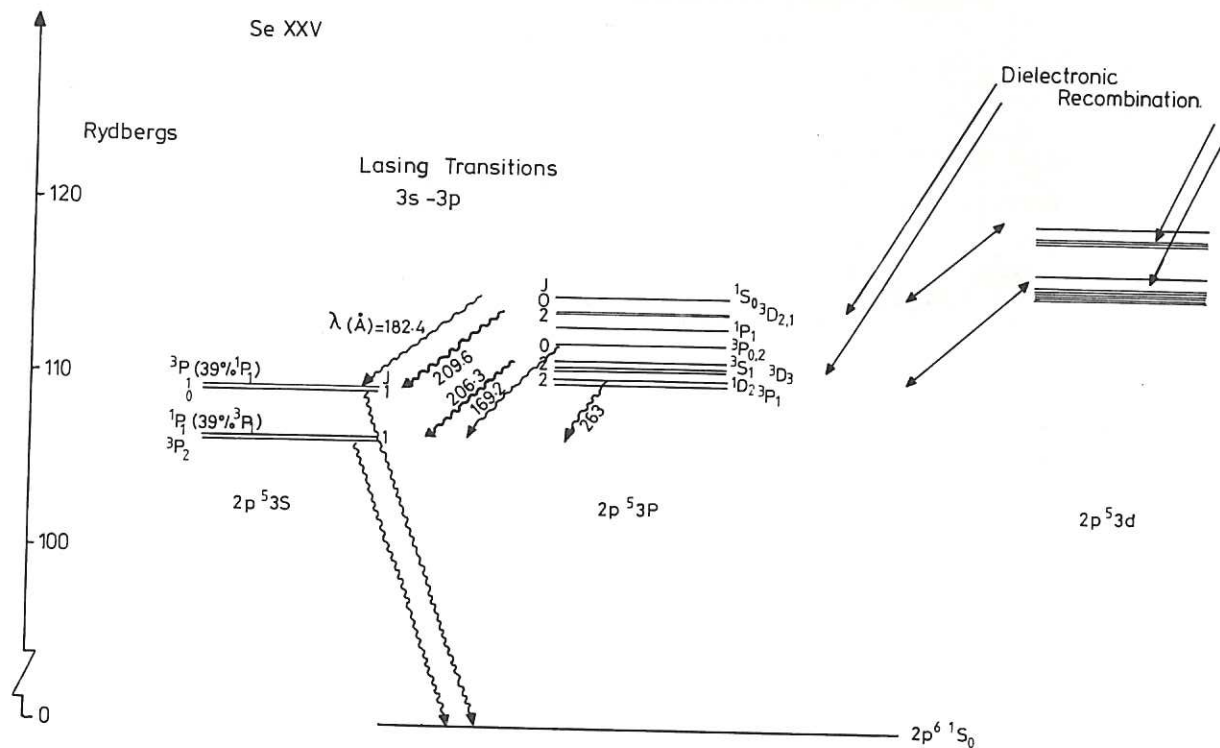


Fig.5 Energy level scheme for Se XXV indicating lasing transitions.

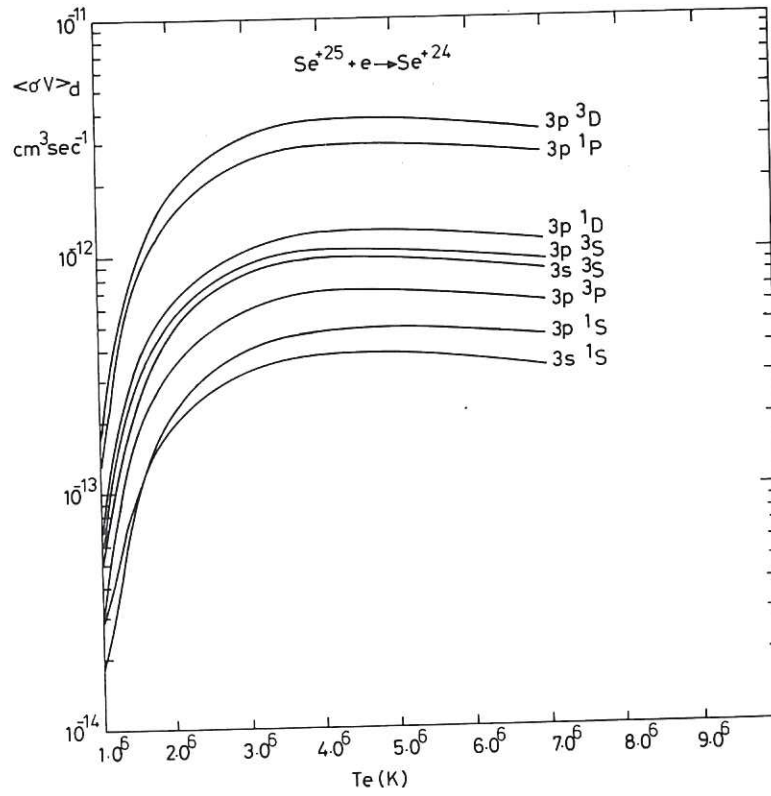


Fig.6 Dielectronic recombination rates $\langle \sigma v \rangle_d$ into $2s^2 2p^5 3p$ levels of Se_{xxv} . Cascade contributions are not included.

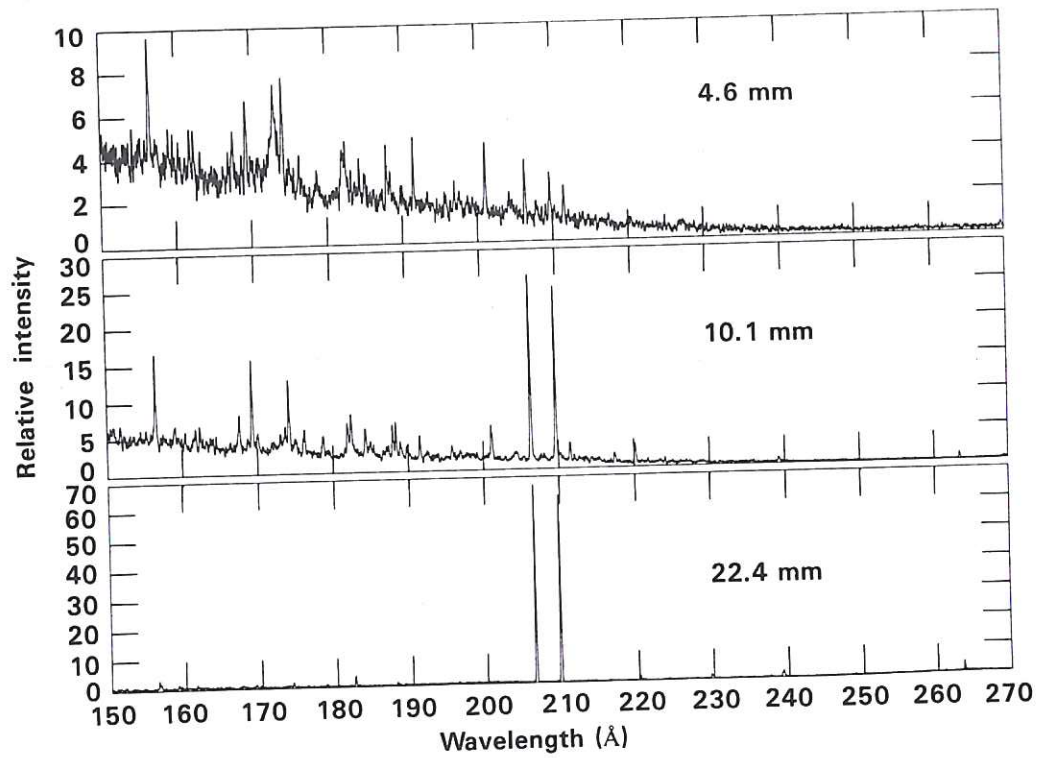


Fig.7 Spectrum from irradiated Se foil target. The intensities of the two lasing transition increase exponentially with gain length. (DL Matthews et al, LLL 1984).

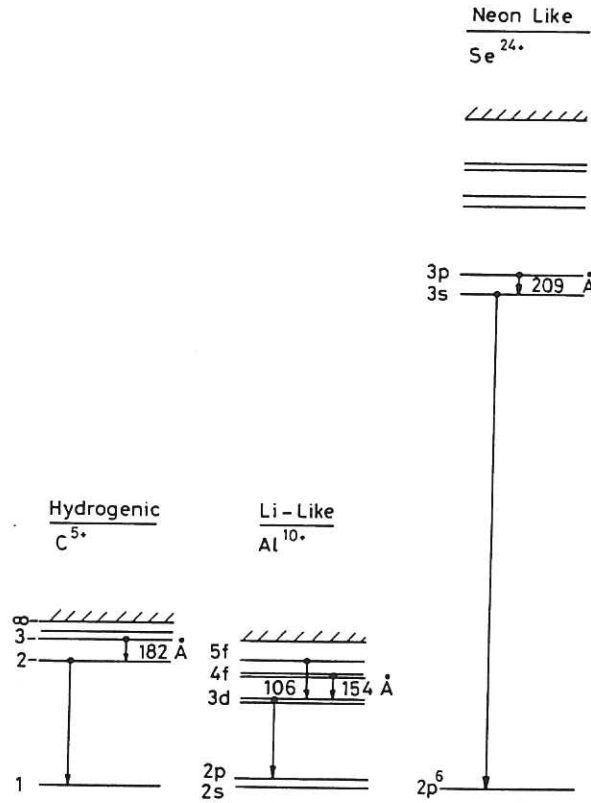


Fig.8 Relative Quantum efficiency of different lasant schemes. The main parameters associated with experimental demonstrations of Gain are appended.

Hydrogenic Ions e.g. C^{5+}

Ref. [4]	$n_e = 2 \times 10^{19} \text{cm}^{-3}$ $T_e = 30 \text{eV}$ $\Phi_p(0.53\mu) 10^{13} \text{Wcm}^{-2} \approx 20 \text{Jcm}^{-1} \approx 0.3 \text{TWcm}^{-1}$ $\alpha(182 \text{\AA}) \approx 4 \text{cm}^{-1}$	free expansion $\tau_{ASE} \approx 0.15 \text{ns}$
Ref. [5]	$n_e \approx 2 \times 10^{19} \text{cm}^{-3}$ $T_e \approx 30 \text{eV}$ $\int \Phi_p(10\mu\text{m}).dt = 300 \text{J}$ $\alpha(182 \text{\AA}) \approx 6.5 \text{cm}^{-1}$	Stagnated expansion, B = 9 Tesla $\tau_{ASE} \approx 50\text{-}100 \text{ns}$

Li-like Ions e.g. Al^{10+}

Ref. [3]	$n_e \approx 1.5 \times 10^{19} \text{cm}^{-3}$ $T_e \approx 30 \text{eV}$ $\Phi_p \approx 6 \times 10^{11} \text{W/cm}^2$ $\alpha(106 \text{\AA}) \sim 2.5 \text{cm}^{-1}$	free expansion $\tau_p \sim 4 \rightarrow 20 \text{ns}$
----------	--	--

Neon-like Ions e.g. Se^{24+}

Ref. [2]	$n_e \approx 8 \times 10^{20} \text{cm}^{-3}$ $T_e \approx 800 \text{eV}$ $\Phi_p(0.53\mu) \approx 5 \times 10^{13} \text{Wcm}^{-2} \approx 500 \text{Jcm}^{-1} \approx 1 \text{TWcm}^{-1}$ $\alpha \sim 5 \text{cm}^{-1}, \alpha L \approx 20, \delta\theta \sim 10 \text{mR.}$ $P_{ASE} \sim 1 \text{MW},$	free expansion $\tau_p \approx 450 \text{ps}$ $\tau_{ASE} \approx 200 \text{ps}$ $E_{ASE} \approx 200 \mu\text{J}$
----------	--	---

Note: subscripts 'p' stands for 'pump power'.
 'ASE' stands for amplified stimulated emission.

